

# **Polymer nanoparticles for the release of fragrances: How the physico-chemical properties influence the adsorption on textile and the delivery of limonene**

*Nicolò Manfredini<sup>1,#</sup>, Juri Ilare<sup>1,#</sup>, Marzio Invernizzi<sup>1</sup>, Elisa Polvara<sup>1</sup>, Daniel Contreras Mejia<sup>1</sup>,  
Selena Sironi<sup>1</sup>, Davide Moscatelli<sup>1</sup>, and Mattia Sponchioni<sup>1,\*</sup>*

<sup>1</sup> Department of Chemistry, Materials and Chemical Engineering, Politecnico di Milano, Via Mancinelli 7 - 20131 Milano, Italy.

<sup>#</sup>Co-first authors

<sup>\*</sup>Corresponding author: Mattia Sponchioni; E-mail: [mattia.sponchioni@polimi.it](mailto:mattia.sponchioni@polimi.it)

**Abstract:** *The market of cosmetic and personal care products is continuously growing its impact. In particular, the products that are currently driving this growth have a strict connection with fragrances (e.g. perfumes, detergents, body creams, and softeners). Since the fragrances are volatile molecules, very often they are encapsulated in polymeric nanoparticles (NPs) that mediate their release and hence prolong the fragrance perception. Towards this aim, it is highly desirable to maximize the interaction between the carrier and the substrate, which would avoid the NP desorption following scrubbing and repeated washings. In the case of laundry products, a limited NP desorption is also crucial to prevent the accumulation of nanoplastics in the environment, which is nowadays strictly regulated. Therefore, a thorough study highlighting the influence of the different physico-chemical properties of the NPs on their adsorption behavior is urgently required.*

*In this work, we synthesized polymer NPs with different size, surface charge, glass transition temperature and cross-linking through emulsion Free-Radical Polymerization (eFRP) to investigate how these parameters affect the NP adsorption onto a textile substrate (composition: 90% cotton – 10% elastane). This study can provide interesting guidelines in the design of new fragrance delivery systems as well as in the optimization of those already adopted in the market. Finally, we investigated the possibility of loading and mediating the release in air of limonene, one of the most common odorous molecules in the cosmetic field, overcoming its well-known volatility.*

**KEYWORDS:** Polymer Nanoparticles; Free-Radical Polymerization; FRP; Adsorption; Laundry; Cosmetic; Fragrance Release; Limonene

## 1. Introduction

According to Global Industry Analyst, Inc.<sup>1</sup>, the market of perfumes, laundry and detergency active compounds is expected to reach US\$ 3.9 billion by 2025, owing to the growing impact in everyday people life. In this scenario, a leading role is played by fragrances, which are present in most of the abovementioned products. In particular, the employment of fragrances is acquiring great interest in food<sup>2</sup>, papermaking<sup>3</sup>, textile industries<sup>4</sup>, cosmetic<sup>5,6</sup>, personal care, and household products<sup>7</sup>.

The choice of the fragrance is generally dictated by the aroma to be imparted to the final product, which in turn depends on the chemical structure of the molecule<sup>8</sup>. Nowadays, linalool and limonene are the most diffused fragrances, being present in more than 50% of the cosmetic products currently available on the market<sup>7,9</sup>. In order to activate the specific area of the central nervous system and to elicit a sensorial response, the odorant molecule needs to reach the nasal receptors<sup>10,11</sup>. Consequently, high vapor pressure and volatility typically characterize fragrances<sup>12</sup>. These peculiarities hamper a long-lasting fragrance perception. For instance, the temperature and pressure variations during the storage may cause the partial loss of the aroma and a subsequent loss in performance during the application. Therefore, to prolong the fragrance perception, such molecules are often loaded in suitable carriers able to mediate their release during time.

Towards this aim, carriers with different morphologies and chemical composition have been developed and reported in the literature. Among them, the most diffuse are micro- and nanocapsules as well as micro- and nanoparticles (NPs). Systems in the nanoscale are often the preferred choice due to their higher specific surface compared to the microparticles, which enables the more efficient fragrance loading in the carrier and subsequent interaction with the substrate. Nanocapsules are appealing for their inner hollow cavity, enabling to host a significant amount of fragrance. Different materials have been reported for the synthesis of the wall, including synthetic polymers, inorganic material and polymer-inorganic composites, reviewed in <sup>2</sup>. However, the complexity in the preparation of such carriers, as well as their limited interaction with the fragrance preventing its sustained release affect the interest towards this morphology in favor of NPs. The same classification based on the constituting materials can be applied to these delivery systems. NPs made up of inorganic silica<sup>13</sup>, metal-organic frameworks<sup>14</sup>, and polymer-inorganic composites<sup>15</sup> have been successfully used to mediate the release of fragrances. However, polymeric nanoparticles (NPs) are among the most investigated carriers, mainly due to their tunable properties, such as size distribution, glass transition temperature and surface charge, which in turn enable the optimization of the

loading efficiency as well as the interaction with the substrate. In particular, polymeric NPs are notably suitable carriers thanks to their low reactivity towards the active species, low viscosity at high concentrations, and good adsorption/desorption properties<sup>7,16-20</sup>. Furthermore, also the encapsulation methodology influences the kinetics of fragrance release depending if the encapsulated molecule can create a chemical or a physical bond with the carrier<sup>6,21,22</sup>.

Within this framework, fragrance delivery by means of polymeric NPs is particularly appealing in the textile field. Indeed, in everyday life, customers desire to preserve as long as possible the odor of suits, pullovers, T-shirts and several other garments after every washing cycle<sup>4,5,23,24</sup>.

To achieve this goal, the interaction between the odorous molecule and the polymeric carrier must guarantee an efficient fragrance loading. Then, the NPs should be properly designed in order to adsorb strongly on the textile, in order to have the chance to release their cargo for a prolonged time.

Despite polymer NPs exhibit high versatility and then enable to meet such criteria, their use is more and more regulated by national and international authorities. In fact, the tendency is currently to favor more environmentally friendly alternatives, with the limitation of plastics and microplastics that accumulate in the environment. In this direction, the European Chemicals Agency (ECHA)<sup>25</sup> will soon propose to limit the utilization of polymers in the cosmetic field only to those able to either: i) degrade in short time, ii) mutate their features going out from the nano- and micro- plastic definitions, or iii) guarantee very low desorption from the substrates. This radical change in direction in the regulatory framework stimulated the research towards biodegradable alternatives to the traditional polymeric fragrance delivery systems<sup>16,26,27</sup>. However, the scarcity of biodegradable NPs, together with their cost, still far from being competitive with the traditional plastics, prevent their diffusion on the market in a short time<sup>28,29</sup>. Hence, rinsing-resistant NPs would combine a prolonged release of the fragrance with the fulfillment of the future regulations in the field of laundry products.

With this framework in mind, in this work we first conducted a comprehensive study on the influence of the most important physico-chemical features, *i.e.* glass transition temperature, nanoparticle size, surface charge, cross-linking degree, of polymer NPs on their adsorption and desorption behavior on a 90% cotton – 10% elastane fabric. First, we produced surfactant-free poly(butyl acrylate) (PBA)-based NPs stabilized with either 2-(methacryloyloxy)ethyl]trimethylammonium chloride (MADQUAT) or 3-sulfopropyl methacrylate potassium salt (SPMAK) *via* free-radical emulsion polymerization (eFRP). In

this way, we were able to investigate the influence of the particle size and their surface charge (*i.e.* positive and negative, respectively) over the adsorption. Then, the cross-linking of the polymer chains constituting the NPs was tested using ethylene glycol dimethacrylate (EGDMA) as cross-linker. Finally, the effect of the glass transition temperature over the adsorption was investigated by comparing NPs made up of poly(butyl acrylate) ( $T_g = -53\text{ }^\circ\text{C}$ ), poly(styrene) ( $T_g = 100\text{ }^\circ\text{C}$ ), or poly(butyl methacrylate) ( $T_g = 20\text{ }^\circ\text{C}$ ). Once optimized the interactions between the polymer NPs and the substrate, we demonstrated the possibility of encapsulating limonene *via* nanoprecipitation using a T-MIXING device. In order to study the release of limonene in air from our carriers, we simulated a washing cycle on a textile substrate and successively analyzed the concentration of limonene released in Nalophan™ bags through gas chromatography (GC). In this way, it was possible to detect the fragrance concentration in air, a key aspect for the final application of these systems. Finally, due to the stringent requirements from the regulatory agencies, the desorption kinetic of these systems from the substrate is presented.

## 2. Materials and methods

### 2.1. Materials

Styrene (STY,  $\geq 99\%$ , MW = 104.15, Sigma Aldrich), butyl acrylate (BA,  $\geq 99\%$ , MW = 128.17, Sigma Aldrich), butyl methacrylate (BMA, 99%, MW = 142.20, Sigma Aldrich), [2-(methacryloyloxy)ethyl]trimethylammonium chloride solution (MADQUAT, 75 % w/w, MW = 207.70, Sigma Aldrich), ethylene glycol dimethacrylate (EGDMA, 98 %, MW = 198.2, Sigma Aldrich), 2,2'-azobis(2-methylpropionamide) dichloride (V-50, 98 %, MW = 271.19, Acros Organics), 3-sulfopropyl methacrylate potassium salt (SPMAK, 98 %, MW = 246.32, Sigma Aldrich), potassium peroxydisulfate (KPS,  $\geq 99\%$ , MW = 270.32, Fluka Chemika), N,N-dimethylformamide (DMF, 99.8 %, MW = 73.09, Sigma Aldrich), limonene (LEM, 90 %, MW = 136.23, Sigma Aldrich), deionized (DI) water were used without further purifications except when specifically indicated. All the solvents were of analytical grade purity and used as received. Nalophan™ bags with polytetrafluoroethylene (PTFE) connections were assembled in-house.

### 2.2. Nanoparticle synthesis

The polymeric NPs investigated in this work were synthesized *via* surfactant-free batch eFRP. To investigate the influence of a different  $T_g$  on the adsorption, we selected STY to produce

hard NPs ( $T_g = 100\text{ }^\circ\text{C}$ ) BMA for NPs with an intermediate  $T_g$  ( $T_g = 20\text{ }^\circ\text{C}$ ) and BA for soft NPs ( $T_g = -53\text{ }^\circ\text{C}$ ). Regarding the tuning of the surface charge, positively charged NPs were synthesized using MADQUAT as surfmer and V-50 as initiator. On the other hand, negatively charged NPs were obtained by adopting SPMAK as surfmer and KPS as initiator. Finally, the introduction of EGDMA in the formulation enabled to obtain cross-linked NPs. The list of the NPs synthesized in this work with their physico-chemical properties is reported in **Table 1**. Herein, M and S indicate NPs produced using MADQUAT or SPMAK as surfmer, respectively. Moreover, cross-linked NPs are differentiated from the non-cross-linked ones through the C reported in the name abbreviation. Finally, the numbers indicate the surfmer/monomer mass ratio.

As a representative synthesis, in the case of M1C (cross-linked NPs synthesized using MADQUAT as surfmer and a surfmer/monomer ratio = 1.0% w/w), a 100 mL septa-sealed round bottom flask equipped with a magnetic stirrer was filled with 45 g of DI water and 0.05 g (1% w/w based on BA) of MADQUAT. The organic phase, composed by 5 g of BA and 0.05 g (1% w/w based on BA) of EGDMA, was promptly mixed and subsequently added to the flask. Then, the mixture was purged for 20 minutes by bubbling nitrogen. The reaction mixture was placed in an oil bath at  $60\text{ }^\circ\text{C}$ , and the reaction was started adding 0.049 g of V-50 dissolved in 5 g of DI water. The polymerization was carried out for 24 hours and the final dispersion was analyzed *via* thermogravimetric analysis, performed on an Ohaus MB35 Moisture Analyser, to evaluate the monomer conversion (**eq. 1**).

$$X(t) = \frac{100 - \%vap(t)}{\%M^0} \quad (1)$$

Here,  $X$  is the conversion,  $\%vap(t)$  is the percentage of the sample taken at time  $t$  that vaporizes during the analysis and  $\%M^0$  is the percentage of monomer in the mixture initially charged in the batch reactor.

The latexes were purified through dialysis carried out for 3 days against distilled water using regenerated cellulose membranes (Spectra\Por, molecular weight cut-off = 3.5 kDa). The dialysis medium was frequently changed to preserve a large concentration gradient. The particle size distribution and the surface charge were characterized *via* dynamic light scattering, performed on a Zetasizer Nano ZS (Malvern Instruments) at a scattering angle of  $173^\circ$ . The measurements were repeated three times, 11 runs each, and the results are the average of the three.

### 2.3. NP adsorption on cotton fabric

Adsorption and desorption investigations were conducted on fabric, used as received, with composition 90% cotton and 10% elastane. 0.5 g of fabric sample were soaked in 50 mL of NP latexes at three different concentrations, namely 0.5, 1 and 2 mg/mL, under mild stirring. The experiments were conducted at 25 °C. The residual NP concentration in the suspension at different times was evaluated according to **eq. 2** by measuring the light absorbance of the suspension at 500 nm by means of a Jasco V-630 UV/Vis spectrometer.

$$C(t) = C_0 \frac{Abs(t)}{Abs_0} \quad (2)$$

Where  $C_0$  is the initial NP concentration and  $Abs(t)$  and  $Abs_0$  are the sample absorbance measured at time  $t$  and time zero, respectively. The linear relationship between the NP concentration in the liquid and its absorbance was verified for all the NP latexes as reported in **Figure S1** for the sample M1C, as an example. To prevent any variation in the volume, the sample was put back in the beaker after every analysis. The specific amount of adsorbed NPs per gram of cotton fabric ( $Q$ ) was quantified according to **eq. 3**<sup>30,26</sup>.

$$Q(t) = \frac{V C_0}{m_c} \left( 1 - \frac{Abs(t)}{Abs_0} \right) \quad (3)$$

Here,  $V$  is the volume of the liquid,  $C_0$  the initial NP concentration, and  $m_c$  the mass of cotton substrate in the experiment.

Since an important component of the light absorbance measured during the experiment is due to the scattering operated by the NPs, which is a function of the NP size and concentration, for the validity of the analysis it is essential that the NPs maintain the same size and hence give the same scattering throughout the whole experiment. Therefore, the NP stability was checked through DLS along the entire adsorption experiment as shown in the example in **Figure S2** for the M1C sample. The preservation of the NP size ensures that the variation in the light absorbance is only imputable to a change in the NP concentration in the liquid phase. A similar procedure was adopted to measure the NP desorption from the substrate. In this case, the pre-loaded textile was immersed in DI water and the NP concentration in the liquid quantified by measuring its absorbance over time following the same **eq. 2**. It is worth

mentioning that in this case  $C_0$  and  $Ab_{s0}$  are the same values used for the adsorption experiments, *i.e.* concentration and related absorbance of the initial NP latex. All of the experiments were conducted in triplicate. After the loading experiment, the fabric sample was dried at 50 °C in an oven for 75 minutes. Scanning electron microscopy (SEM) was conducted to visualize the NPs adsorbed on the textile. Micrographs were taken at an electron high tension (EHT) of 10.00 kV on a Zeiss EVO 50 XVP microscope at a magnification of 5 kX.

#### 2.4. Limonene loading and release

The limonene was encapsulated in the synthesized NPs exploiting the high turbulence created by means of a micromixing device. In order to create a turbulence degree able to favor the diffusion of the fragrance into the NPs, two streams were pumped in two opposite directions and the final dispersion recovered at the outlet of the mixing device. Additionally, the introduction of dimethylformamide (DMF) allowed the pre-swelling of the polymeric NPs in order to facilitate the diffusion of limonene in the core. In details, limonene was dissolved in DMF with a concentration of 20% v/v. 15 mL of NP latex at 5% w/w and 2.5 mL of limonene solution were loaded into two different syringes. The mixtures were fed in one minute to the two extremities of a micromixer (*i.e.* T-MIXER) using two syringe pumps (New Era Pump Systems, NE-300). The loaded NPs were dialyzed against DI water for 1 h using regenerated cellulose membranes (Spectra\Por, molecular weight cut-off = 3.5 kDa) to remove the organic solvent and then adsorbed on the textile by soaking it in the NP latexes for 4 h. After 4 h, the wet fabric was dried in an oven at 50 °C for 75 minutes and successively placed into a Nalophan<sup>TM</sup> bag. The bag was filled with 1 L of nitrogen using a mass flow meter (Alicat Scientific, Tucson, USA). Nalophan<sup>TM</sup> bags made in this way were stored at room temperature for 24 hours and, subsequently, analyzed by GC. A DANI MASTER GC - fast gas chromatograph equipped with a flame ionization detector was used for sample analysis. A methyl polysiloxane capillary column (MEGA s.r.l, Legano, Italy) 20 m, 0.18 mm, with a film thickness of 1 µm was used during the analysis. The carrier gas was helium at a flow rate of 0.8 mL/min. A volume of 0.1 mL of gas was taken from the bags by a 1 mL SGE gas tight syringe and injected into the GC. The temperatures for the injector and detector were 250 and 280 °C, respectively. The temperature program was isothermal for 1 min at 70 °C, raised to 150 °C at a rate of 20 °C/min and isothermal for 1 min. Calibration standards were prepared by evaporation of 0.5 µL of a solution of limonene (8420 µg/mL) in ethanol injected into Nalophan<sup>TM</sup> bags, filled with known volumes of nitrogen and immediately analyzed. The

retention time of limonene is 5.14 min. Quantification values were expressed as parts per million on a volume basis (ppmV). The calibration curve is reported in **Figure S3**.

### 3. Results and discussion

#### 3.1. Characterization of the synthesized NPs

With the aim of studying the influence of different physico-chemical properties over the NP adsorption on cotton-elastane textile, we synthesized NPs with different size, surface charge, cross-linking and Tg. The samples produced in this work, together with their characteristics, are listed in **Table 1** (for a detailed description of the nomenclature the reader is referred to Section 2.2).

**Table 1:** *Properties of the NPs synthesized in this work: size, polydispersity index (PDI), monomer conversion (X), surface charge ( $\zeta$ -potential), surfmer/monomer and EGDA/monomer ratios.*

Sample	Size [nm]	PDI [-]	X [%]	$\zeta$ - potential [mV]	Surfmer/ Monomer [% w/w]	EGDMA/ Monomer [% w/w]
M1	495.0 $\pm$ 3	0.014 $\pm$ 0.005	99	+ 42 $\pm$ 3	1.0	-
M2.5	332.0 $\pm$ 5	0.092 $\pm$ 0.001	96	+ 39 $\pm$ 7	2.5	-
M5	229.0 $\pm$ 3	0.059 $\pm$ 0.003	97	+ 38 $\pm$ 5	5.0	-
M7.5	167.0 $\pm$ 9	0.053 $\pm$ 0.003	95	+ 37 $\pm$ 4	7.5	-
M1C	507.0 $\pm$ 2	0.064 $\pm$ 0.004	98	+ 41 $\pm$ 6	1.0	1
M2.5C	304.5 $\pm$ 6	0.082 $\pm$ 0.005	95	+ 37 $\pm$ 6	2.5	1
M5C	228.0 $\pm$ 5	0.041 $\pm$ 0.007	97	+ 36 $\pm$ 2	5.0	1
M7.5C	137.2 $\pm$ 3	0.011 $\pm$ 0.001	94	+ 35 $\pm$ 3	7.5	1
S0.5	361.0 $\pm$ 7	0.079 $\pm$ 0.005	99	- 41 $\pm$ 8	0.5	-
S1	147.9 $\pm$ 9	0.006 $\pm$ 0.006	98	- 38 $\pm$ 6	1.0	-
S2.5	94.0 $\pm$ 3	0.085 $\pm$ 0.002	99	- 37 $\pm$ 4	2.5	-
S5	85.0 $\pm$ 3	0.059 $\pm$ 0.005	97	- 38 $\pm$ 7	5.0	-
S1C	287.9 $\pm$ 9	0.091 $\pm$ 0.003	96	- 40 $\pm$ 9	1.0	1
S2.5C	195.3 $\pm$ 5	0.012 $\pm$ 0.003	97	- 41 $\pm$ 3	2.5	1
S5C	103.7 $\pm$ 4	0.045 $\pm$ 0.001	98	- 36 $\pm$ 2	5.0	1

S10C	76.1 ± 4	0.100 ± 0.006	97	- 38 ± 5	10.0	1
MSTY1	484.0 ± 7	0.070 ± 0.008	98	+ 41 ± 7	1.0	-
MBMA1	489.3 ± 10	0.081 ± 0.006	97	+39 ± 7	1.0	-

---

In particular, with the eFRP conducted in the presence of a suitable surfmer, a chemical specie behaving both like a monomer and a surfactant<sup>31</sup>, we were able to produce narrowly dispersed NPs (PDI<0.1) without the need for additional surfactants. The narrow particle size distribution (PSD) is extremely important to guarantee the reliability of the adsorption tests. In fact, a broad PSD may lead to competitive adsorption phenomena among particles with different size, thus preventing a clear understanding of the effect of the other parameters. The advantage of using a surfmer is its chemical incorporation in the polymer chains, which prevents any possible desorption from the NP surface once in contact with the textile, which could lead to the latex destabilization.

The choice of the surfmer enables tuning the NP surface charge. In particular, the samples produced using MADQUAT (M1 to M7.5, M1C to M7.5C, MSTY1 and MBMA1 in **Table 1**), show a highly positive charge (*i.e.*  $\zeta$ -potential > +35 mV). On the other hand, the colloids containing SPMAC (S0.5 to S5 and S1C to S10C in **Table 1**) are highly negative (*i.e.*  $\zeta$ -potential < -35 mV). In addition, the NP size can be finely tuned by modulating the surfmer/monomer ratio. In particular, as for traditional surfactants, the higher the surfmer/monomer ratio, the higher the number of nucleated NPs and in turn the smaller their size. Then, by acting on this parameter, we could produce NPs with average size in the range 90 – 500 nm, which allowed the investigation of the effect of the size over the adsorption on the substrate.

Within this size range, we synthesized both non-cross-linked (M1 to M7.5 and S0.5 to S5 in **Table 1**) and chemically cross-linked (M1C to M7.5C and S1C to S10C in **Table 1**) NPs as well as NPs with different Tg (MSTY1 and MBMA1 in **Table 1**), to assess the influence of the polymer rigidity on the adsorption.

### 3.2. Influence of the NP properties over the adsorption/desorption processes

First, we investigated the effect of a different surface charge by studying the adsorption of positive and negative NPs with similar size.

The amount of adsorbed NPs per gram of cotton once the adsorption equilibrium is reached (*i.e.* after 4 hours), indicated as  $Q_e$  and calculated with **eq. 3**, is reported as a function of the residual NP concentration in the suspension (**eq. 2**) at equilibrium ( $C_e$ ), in **Figure 1** for

negatively and positively charged NPs with similar size. The study is conducted both in the case of non-cross-linked (**Figure 1a**) and in the case of cross-linked NPs (**Figure 1b**).

The NP stability was verified every time as described in Section 2.2.

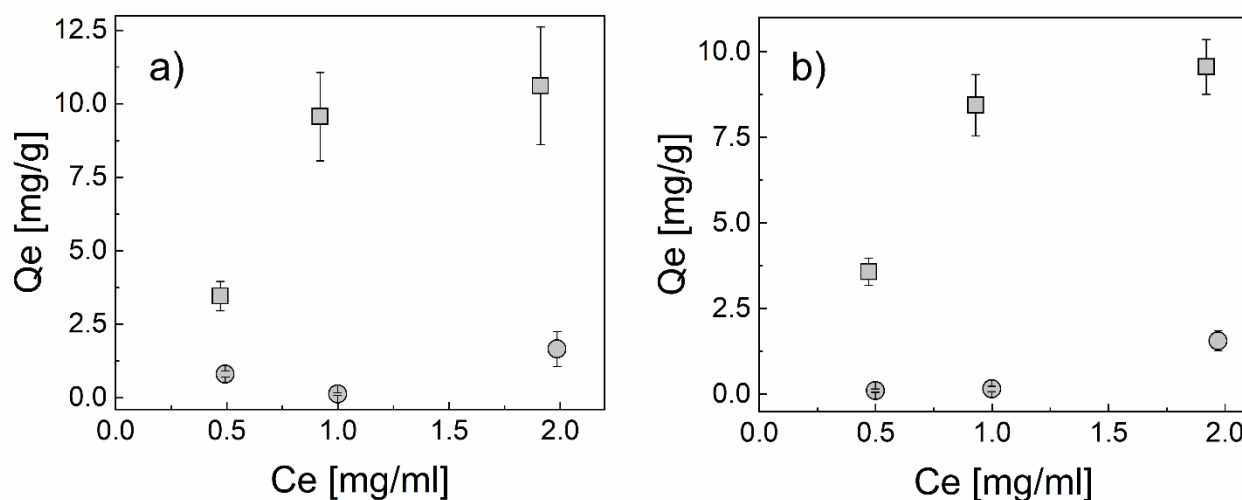


**Figure 1:** Adsorption isotherms of M7.5 (square) and S1 (circle) in the case of the non-cross-linked NPs (a) and M5C (square) and S2.5C (circle) in the case of the cross-linked NPs (b).

As it can be retrieved from the graphs, there is a significant difference in the adsorption between the negatively and positively charged NPs at all the concentrations tested. In particular, the positive NPs lead to Qe as high as 10 mg/g, one order of magnitude higher compared to their negative counterparts.

This difference occurs independently whether the particles are cross-linked or not and is reflected in two different isotherm shapes. In fact, while the positively charged NPs present a favorable isotherm (Langmuir type), the negatively charged ones have the opposite behavior (anti - Langmuir).

These results, quite expected considering that the cotton - elastane (90% - 10%) fabric shows an overall negative charge at neutral pH (an isoelectric point of 2.9 is reported for cotton textiles<sup>32</sup>), suggest that the electrostatic interaction is a fundamental driving force in this kind of processes.

For all the discussed reasons, the negatively charged NPs will not be considered any further. A more detailed study on the impact of other parameters in the interaction between the MADQUAT-based NPs and the cotton-elastane fabric was performed.

First, the kinetic of adsorption for this class of systems was analyzed at three different concentrations, namely 0.5, 1 and 2 mg/mL. The results are reported in **Figure 2a-b** in the case of the M1 and M1C samples, respectively.

As it can be seen in **Figure 2a**, the equilibrium is reached within the first 2 hours at all the concentrations tested. Such a long equilibration time was already reported in the literature for polymeric NPs and is in contrast with the faster adsorption kinetic of small molecules<sup>26,30,33</sup>. Furthermore, the kinetic profile and the time necessary to reach the equilibrium conditions resulted to be the same independently of the NP size, as can be seen in **Figure S4**. Additionally, no significant changes in terms of adsorption rate have been noticed in the case of cross-linked NPs as shown in **Figure 2b**. Moreover, the higher the initial NP concentration, the higher  $Q_e$ , confirming that the adsorption isotherm is of the Langmuir type, as clearly shown in **Figure 2c**.

In addition, a slight difference in terms of mass of NPs adsorbed per gram of cotton has been observed between the cross-linked and non-cross-linked NPs, with the former leading to a higher  $Q_e$ , as shown in **Figure 2c**. This result is quite surprising, since we expected to see a reduction in the NP adsorption with the cross-linking, due to the increase in the polymer rigidity<sup>34</sup>. However, it is worth mentioning that the introduction of cross-links likely increases the NP density, which might favor the NP interactions with the substrate, thus leading to a higher  $Q_e$ .

The expected reduction in the amount of adsorbed NPs at increasing polymer rigidity was evident when comparing positively charged NPs synthesized with different  $T_g$  (**Figure 2d**, M1, STY1 and MBMA1). In particular, the soft PBA-based NPs ( $T_g = -53\text{ }^\circ\text{C}$ ) adsorbed almost 10 times more compared to their hard STY-based counterparts ( $T_g = 100\text{ }^\circ\text{C}$ ) with comparable size. In this case, the interaction of the different side groups in the polymer chains with the substrate could have a role in the adsorption and may prevent to attribute this large difference in  $Q_e$  solely to the difference in  $T_g$ . Therefore, we synthesized PBMA NPs ( $T_g = 20\text{ }^\circ\text{C}$ ) with similar size, surface charge and side groups as those of M1. Also in this case, a higher  $T_g$  led to a significant drop in  $Q_e$  compared to PBA-based NPs.

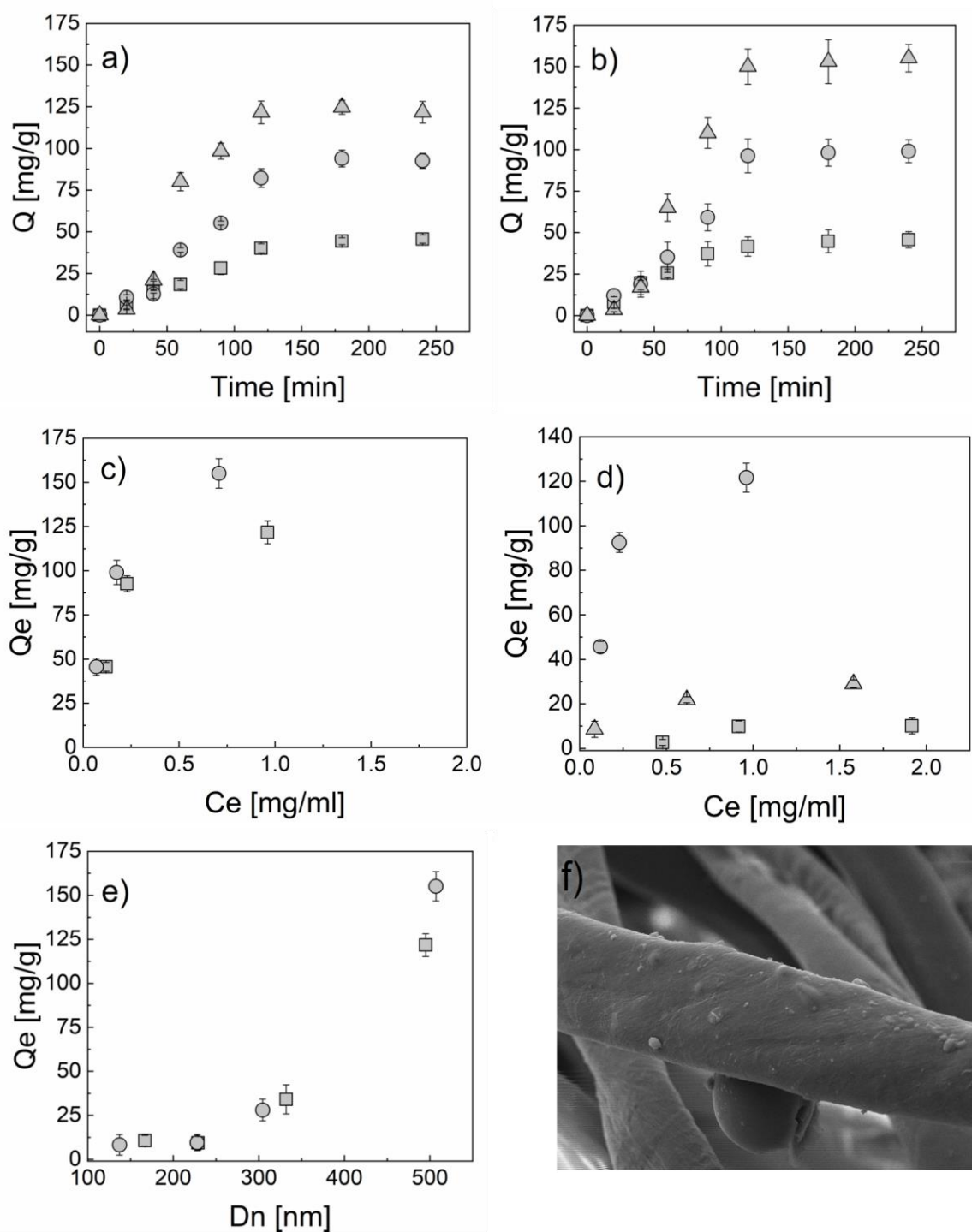


**Figure 2:** (a) Adsorption kinetic in the case of MI at 0.5 (square), 1 (circle) and 2 (triangle) mg/mL. (b) Adsorption kinetic in the case of MIC at 0.5 (square), 1 (circle) and 2 (triangle) mg/mL. (c) Adsorption isotherms of MI (square) and MIC (circle). (d) Adsorption Isotherms of MI (circle), MBMAI (triangle) and MSTYI (square). (e)  $Q_e$  as a function of the NP size ( $D_n$ ) in the case of non-cross-linked NPs (square) and cross-linked NPs (circle) adsorbed at an initial concentration of 2 mg/mL. (f) SEM image of a cotton-elastane fiber loaded with MI at 2 mg/mL.

This allowed concluding that the plasticity of the PBA-based NPs may determine a favorable deformation and spreading of the NPs once in contact with the cotton fibers, thus increasing the number of reactive collisions responsible for the adsorption onto the surface. On the other

hand, a NP with high Tg has a more rigid structure that prevents the latter phenomenon reducing the efficacy of the interactions and thus the amount of NPs finally present on the surface.

However, this phenomenon was not observed in the case of the cross-linked NPs, at least at the concentration used in this study. A possible explanation of this could be the low amount of cross-linker added during the synthesis that may had not changed significantly the final Tg of the polymer.

It is worth mentioning that our goal was not to stress this phenomenon but to evaluate if, with the quantities commonly employed in industrial processes, the cross-linker would have had an effect on the NP adsorption and fragrance release. For this reason, NPs with an increased amount of cross-linker were not synthesized.

Finally, the effect of the NP size on the adsorption has been evaluated for both the cross-linked and non-cross-linked NPs, as shown in **Figure 2e**, in the case of a NP concentration during the adsorption of 2 mg/mL. Similar trends were obtained also for different concentrations, as reported in **Figure S5**.

We found an exponential increase in  $Q_e$  with the NP size, reaching a plateau only at  $D_n < 200$  nm. Moreover, there is not a huge difference between the cross-linked and non-cross-linked NPs, confirming what described above. This trend could be justified assuming a constant and limited number of available active sites, well distributed onto the fabric. In fact, if this were the case, the same number of polymeric NPs would be adsorbed on the textile, independently from their size. Then, considering that the densities of the NPs are comparable, the bigger the NP the higher the mass of polymer adsorbed on the fabric, as reported in **Figure 2e**.

The effective presence of the NPs on the textile surface was further confirmed by the SEM micrograph reported in **Figure 2f**. In particular, the micrograph confirms that the NPs preserve the spherical shape after adsorption and do not form aggregates on the cotton fibers.

Lastly, the capability of these systems to desorb from the fabric when washed in fresh water was evaluated. This test is important to understand if these systems are suitable to grant a prolonged fragrance release from the substrate as well as if they fall into the European Union restrictions in the use of microplastics in laundry and cosmetic products, as already described in the introduction.

In particular, the amount of NPs present in the liquid phase after the desorption is calculated with the procedure described in Section 2.2 using the same **eq. 2** employed for the evaluation of the NP concentration in the adsorption process. In this way, it was possible to calculate the

amount of NPs still present on the cotton surface during the desorption process ( $Q_{des}$ , eq. S1), as shown in **Figure 3** in the case of the M1 sample.

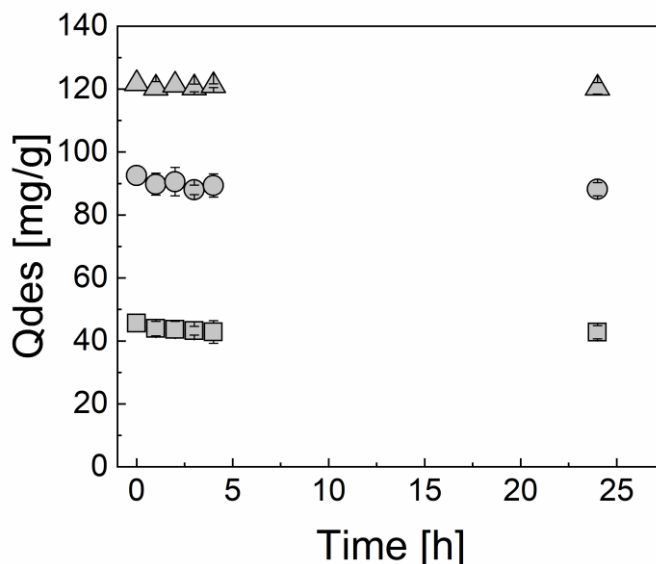


**Figure 3:** Amount of NPs adsorbed onto the fabric during the desorption process ( $Q_{des}$ ) in the case of M1 previously adsorbed at 0.5 (square), 1 (circle) and 2 (triangle) mg/mL.

It is worth mentioning that all the NPs show a similar trend with a maximum desorption below the 7%, as reported in **Table S1**. Looking at the table, it is possible to see that the desorption is independent of the NP size and cross-linking, indicating the irreversibility of the adsorption. This behavior allows the applicability of these NPs in laundry products, falling into the third possibility previously mentioned and described by the ECHA<sup>25</sup>. This result is even more important if we compare the costs of the systems developed in this work and that of equivalent biodegradable carriers<sup>26</sup>. In fact, comparing them at a fixed initial suspension concentration (*i.e.* 1 mg/mL) and  $Q_e$  (*i.e.* 100 mg/g), we noticed that the cost of the latter is almost 25 times higher than the former. More in detail, the biodegradable systems have a price of 0.068 \$ per gram of textile while the non-biodegradable ones of 0.0031\$. Therefore, even if biodegradable laundry products are attracting significant research effort to contain the accumulation of plastics, they are still far from being economically competitive with the traditional solutions. Hence, optimized fragrance delivery systems enabling to satisfy the more and more stringent regulations from the authorities represent the only sustainable laundry products until a viable production scale-up for biodegradable carriers is developed.

In any case, it is worth mentioning that this study is not aimed at proposing new formulations to be applied in laundry products but rather at clarifying the crucial role of the NP physico-

chemical properties in driving their adsorption on synthetic textile. The considerations elaborated in this work can be regarded as guidelines in the optimization of novel NPs, substituting for example the poly(BA) with a biodegradable polymer, which should share a similar low Tg (*e.g.* poly(caprolactone)) while keeping constant the other parameters of the best performing samples.

### 3.3. Limonene release test

The ability of the NPs to encapsulate and release an appreciable amount of limonene was tested in the case of all the MADQUAT-based particles at two different adsorption concentrations, namely 1 and 2 mg/mL. Furthermore, a test with one negatively charged NP has been performed as well.

In **Figure 4**, we show the cumulative limonene release in a Nalophan<sup>TM</sup> bag in static conditions as a function of the NP size. The limonene concentration is represented in ppm in N<sub>2</sub> and is calculated from the calibration curve reported in **Figure S3**.

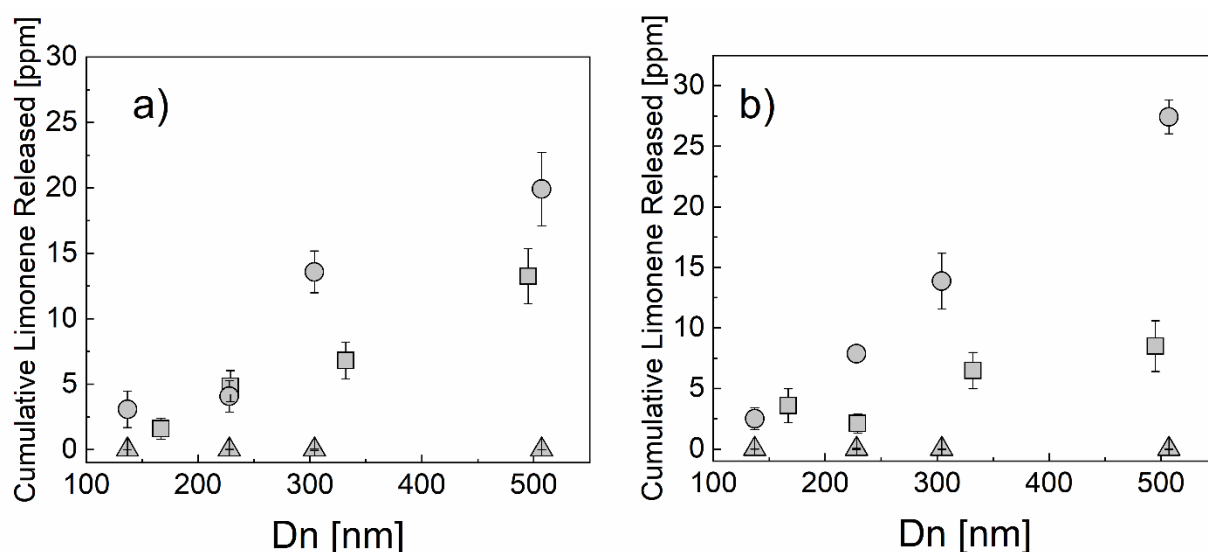


**Figure 4:** Cumulative limonene released as a function of NP size in the case of positively charged NPs at the adsorption concentration of 1 mg/ml (a) and 2 mg/ml (b) for non-cross-linked (square) and cross-linked (circle) NPs and limonene alone (triangle).

When limonene is not encapsulated in polymer NPs, its concentration in the bag is negligible, thus testifying that it is entirely lost during the drying of the textile. Therefore, proper fragrance carriers are required to enable the fragrance perception, acting against its volatility. In particular, the NPs proposed herein worked well in this direction, enabling the limonene detection by GC-FID even after drying the textile at 50 °C.

More specifically, as shown in **Figure 4**, the bigger the NPs, the higher the limonene concentration in the bag, reflecting the higher NP loading on the textile (**Figure 2**).

However, the difference seems to be modest if compared to the exponential function relating  $Q_e$  with the NP size shown in **Figure 2**. This could be explained considering that the smaller the NPs the higher the total surface area, when the polymer concentration and density are fixed. This could facilitate the limonene encapsulation inside the small NPs. In fact, analyzing the limonene concentration in the bag at the equilibrium (*i.e.* after all the limonene has been released) and knowing the theoretical maximum amount of limonene that could be detected (**eq. S3-S5**), it was possible to calculate the theoretical encapsulation efficiency (expressed as Loading efficiency in **eq. S6**) for all the NPs.

The results shown in **Table S2** confirm the high loading efficiency of the small NPs, proximal to 100%. On the other hand, the big NPs reach lower values of encapsulation with a maximum loading efficiency of 80%. The fact that the small NPs present limonene loading efficiencies close to 100% underlines the suitability of these systems in loading and mediating the fragrance release. In fact, they allow the release of a negligible amount of encapsulated limonene even under harsh drying conditions to which the textile was subjected.

Despite the similar values of adsorbed NPs on the fabric (**Figure 2**), the cross-linked particles release a bigger amount of fragrance. This could be due to the higher capability of these NP to encapsulate the limonene.

Nevertheless, the amount of limonene released is significantly higher than in the case of the negatively charged NPs (**Figure S6**) for all the positively charged NPs, which reflects the poor adsorption of negatively charged NPs on the textile.

It is worth mentioning that in all of the cases the limonene concentration in the bag is well above the concentration of 1.8 ppb. This is reported as the minimum concentration required for the limonene to be detected by the human nose<sup>35</sup>.

Finally, the big NPs seem to be the more suitable for guaranteeing good performances in terms of both adsorption and fragrance release. Moreover, the poor desorption values, in line with the future potential EHCA restrictions, coupled with the competitive price of these systems, pave the way for the possible future commercialization of these carriers.

#### 4. Conclusions

In this study, we analyzed the interaction of polymeric NPs with a 90% cotton – 10% elastane textile. Our aim was to highlight how the different physico-chemical properties like surface

charge, glass transition temperature ( $T_g$ ), size and degree of cross-linking impact the adsorption of the NPs, which are widely adopted on the market for the encapsulation and controlled release of volatile fragrances. The surface charge resulted to be the most important parameter in driving the adsorption, with the positively charged NPs showing higher  $Q_e$  than their negative counterparts, mainly due to the overall negative surface of the cotton fibers. The favorability of the process is underlined by the Langmuir type isotherm of these NPs. Moreover, the cross-linking degree, at least at the concentration used in this study, seems not to change significantly the amount of NPs adsorbed on the textile. On the other hand, the  $T_g$  plays a key role, with soft PBA NPs adsorbing more compared to the harder PBMA and STY NPs.

Finally, bigger NPs resulted to be better in terms of adsorption but worse in terms of limonene encapsulation efficiency than the smaller ones. In any case, the limonene released is well above the minimum detectable concentration for all the positively charged NPs tested, paving the way to a possible future commercial application of these carriers. Lastly, the poor desorption of these systems is in line with the future restrictions in the use of NPs in laundry and cosmetic products that the European Chemicals Agency will propose.

### **Author contribution**

N. M. and J. I. equally contributed to the work

### **Declaration of Competing Interests**

The authors declare no conflict of interests.

### **Acknowledgments**

The authors are grateful to Mariasole Morandini for her contribution to the syntheses and characterization of the NPs.

### **Supporting Information**

Electronic supporting information reporting the linear relationship between light absorbance and NP concentration, calibration curve for limonene, adsorption kinetics for positively charged NPs,  $Q_e$  as a function of  $D_n$  for cross-linked and non-cross-linked positive NPs, maximum desorption for the same NPs and limonene loading efficiency for the produced NPs are available at the publisher's website.

## References

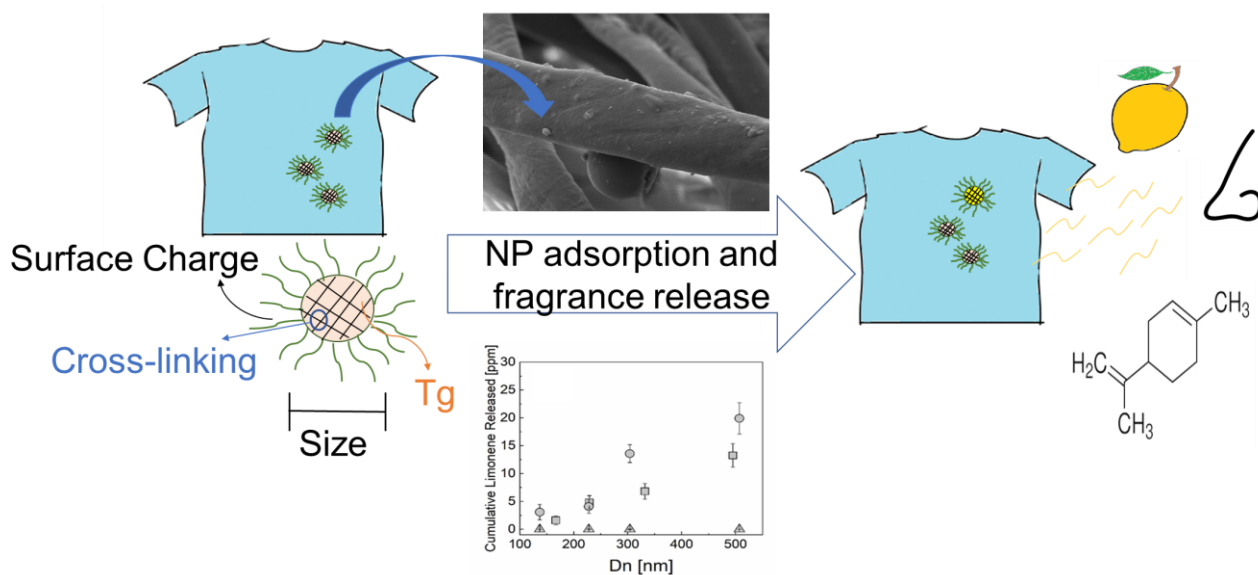
- (1) Global Industry Analysts, I. Active Ingredients for Cosmetics - Market Analysis, Trends, and Forecasts.
- (2) He, L.; Hu, J.; Deng, W. Preparation and Application of Flavor and Fragrance Capsules. *Polym. Chem.* **2018**, *9* (40), 4926–4946. <https://doi.org/10.1039/c8py00863a>.
- (3) Ichiura, H.; Takayama, M.; Nishida, N.; Otani, Y. Interfacial Polymerization Preparation of Functional Paper Coated with Polyamide Film Containing Volatile Essential Oil. *J. Appl. Polym. Sci.* **2012**, *124* (1), 242–247. <https://doi.org/10.1002/app.33900>.
- (4) Hu, J.; Chen, M.; Xiao, Z.; Zhang, J. Sustained-Release Properties of Cotton Fabrics Impregnated with Nanotuberoses Fragrance. *J. Appl. Polym. Sci.* **2015**, *132* (12), 1–9. <https://doi.org/10.1002/app.41678>.
- (5) Hu, J.; Xiao, Z.; Zhou, R.; Li, Z.; Wang, M.; Ma, S. Synthesis and Characterization of Polybutylcyanoacrylate-Encapsulated Rose Fragrance Nanocapsule. *Flavour Fragr. J.* **2011**, *26* (3), 162–173. <https://doi.org/10.1002/ffj.2039>.
- (6) Günay, K. A.; Benczedi, D.; Herrmann, A.; Klok, H. A. Peptide-Enhanced Selective Surface Deposition of Polymer-Based Fragrance Delivery Systems. *Adv. Funct. Mater.* **2017**, *27* (2). <https://doi.org/10.1002/adfm.201603843>.
- (7) Kaur, R.; Kukkar, D.; Bhardwaj, S. K.; Kim, K.; Deep, A. Potential Use of Polymers and Their Complexes as Media for Storage and Delivery of Fragrances. *J. Control. Release* **2018**, *285* (July), 81–95. <https://doi.org/10.1016/j.jconrel.2018.07.008>.
- (8) VDI. VDI 3882 BLATT 2 Olfactometry - Determination of Hedonic Odour Tone. 1994, p 19.
- (9) Bartsch, J.; Uhde, E.; Salthammer, T. Analysis of Odour Compounds from Scented Consumer Products Using Gas Chromatography-Mass Spectrometry and Gas Chromatography-Olfactometry. *Anal. Chim. Acta* **2016**, *904*, 98–106. <https://doi.org/10.1016/j.aca.2015.11.031>.
- (10) Sankaran, S.; Khot, L. R.; Panigrahi, S. Biology and Applications of Olfactory Sensing System: A Review. *Sensors Actuators, B Chem.* **2012**, *171–172*, 1–17. <https://doi.org/10.1016/j.snb.2012.03.029>.
- (11) Gane, S.; Georganakis, D.; Maniati, K.; Vamvakias, M.; Ragoussis, N.; Skoulakis, E. M. C.; Turin, L. Molecular Vibration-Sensing Component in Human Olfaction. *PLoS One* **2013**, *8* (1). <https://doi.org/10.1371/journal.pone.0055780>.
- (12) Buettner, A. *Springer Handbook of Odor*; 2017. <https://doi.org/10.1007/978-3-319-26932-0>.
- (13) Liu, Y.; Wang, Y.; Huang, J.; Zhou, Z.; Zhao, D.; Jiang, L.; Shen, Y. Encapsulation and Controlled Release of Fragrances from Functionalized Porous Metal–Organic Frameworks. *AIChE J.* **2019**, *65* (2), 491–499. <https://doi.org/10.1002/aic.16461>.

- (14) Zhang, B.; Huang, J.; Liu, K.; Zhou, Z.; Jiang, L.; Shen, Y.; Zhao, D. Biocompatible Cyclodextrin-Based Metal-Organic Frameworks for Long-Term Sustained Release of Fragrances. *Ind. Eng. Chem. Res.* **2019**, *58* (43), 19767–19777. <https://doi.org/10.1021/acs.iecr.9b04214>.
- (15) Rehan, M.; El-Naggar, M. E.; Mashaly, H. M.; Wilken, R. Nanocomposites Based on Chitosan/Silver/Clay for Durable Multi-Functional Properties of Cotton Fabrics. *Carbohydr. Polym.* **2018**, *182*, 29–41. <https://doi.org/10.1016/j.carbpol.2017.11.007>.
- (16) Martins, I. M.; Barreiro, M. F.; Coelho, M.; Rodrigues, A. E. Microencapsulation of Essential Oils with Biodegradable Polymeric Carriers for Cosmetic Applications. *Chem. Eng. J.* **2014**, *245*, 191–200. <https://doi.org/10.1016/j.cej.2014.02.024>.
- (17) Velmurugan, P.; Ganeshan, V.; Nishter, N. F.; Jonnalagadda, R. R. Encapsulation of Orange and Lavender Essential Oils in Chitosan Nanospherical Particles and Its Application in Leather for Aroma Enrichment. *Surfaces and Interfaces* **2017**, *9* (September), 124–132. <https://doi.org/10.1016/j.surfin.2017.08.009>.
- (18) Abadie, M. J. M.; Voytekunas, V. Y.; Rusanov, A. L. State of the Art Organic Matrices for High Performance Composites: A Review. *Iran. Polym. J.* **2006**, *15* (1), 65–77.
- (19) Hofmeister, I.; Landfester, K.; Taden, A. PH-Sensitive Nanocapsules with Barrier Properties: Fragrance Encapsulation and Controlled Release. *Macromolecules* **2014**, *47* (16), 5768–5773. <https://doi.org/10.1021/ma501388w>.
- (20) Ferrari, R.; Talamini, L.; Violatto, M. B.; Giangregorio, P.; Sponchioni, M.; Morbidelli, M.; Salmona, M.; Bigini, P.; Moscatelli, D. Biocompatible Polymer Nanoformulation To Improve the Release and Safety of a Drug Mimic Molecule Detectable via ICP-MS. *Mol. Pharm.* **2017**, *14* (1), 124–134. <https://doi.org/10.1021/acs.molpharmaceut.6b00753>.
- (21) Ciriminna, R.; Pagliaro, M. Sol-Gel Microencapsulation of Odorants and Flavors: Opening the Route to Sustainable Fragrances and Aromas. *Chem. Soc. Rev.* **2013**, *42* (24), 9243–9250. <https://doi.org/10.1039/c3cs60286a>.
- (22) Zhu, G. Y.; Xiao, Z. B.; Zhou, R. J.; Yi, F. P. Fragrance and Flavor Microencapsulation Technology. *Adv. Mater. Res.* **2012**, *535–537*, 440–445. <https://doi.org/10.4028/www.scientific.net/AMR.535-537.440>.
- (23) Zhao, D.; Jiao, X.; Zhang, M.; Ye, K.; Shi, X.; Lu, X.; Qiu, G.; Shea, K. J. Preparation of High Encapsulation Efficiency Fragrance Microcapsules and Their Application in Textiles. *RSC Adv.* **2016**, *6* (84), 80924–80933. <https://doi.org/10.1039/c6ra16030a>.
- (24) Tekin, R.; Bac, N.; Erdogmus, H. Microencapsulation of Fragrance and Natural Volatile Oils for Application in Cosmetics, and Household Cleaning Products. *Macromol. Symp.* **2013**, *333*

- (1), 35–40. <https://doi.org/10.1002/masy.201300047>.
- (25) ECHA. Regulation cosmetics.
- (26) Capasso Palmiero, U.; Ilare, J.; Romani, C.; Moscatelli, D.; Sponchioni, M. Surfactant-Free and Rinsing-Resistant Biodegradable Nanoparticles with High Adsorption on Natural Fibers for the Long-Lasting Release of Fragrances. *Colloids Surfaces B Biointerfaces* **2020**, *190*, 110926. <https://doi.org/10.1016/j.colsurfb.2020.110926>.
- (27) Masood, M. T.; Zahid, M.; Goldoni, L.; Ceseracciu, L.; Athanassiou, A.; Bayer, I. S. Highly Transparent Polyethylcyanoacrylates from Approved Eco-Friendly Fragrance Materials Demonstrating Excellent Fog-Harvesting and Anti-Wear Properties. *ACS Appl. Mater. Interfaces* **2018**, *10* (40), 34573–34584. <https://doi.org/10.1021/acsami.8b10717>.
- (28) Moscatelli, D.; Sponchioni, M. Bioresorbable Polymer Nanoparticles in the Medical and Pharmaceutical Fields. In *Bioresorbable Polymers for Biomedical Applications*; Elsevier, 2017; pp 265–283. <https://doi.org/10.1016/B978-0-08-100262-9.00012-4>.
- (29) Cingolani, A.; Casalini, T.; Caimi, S.; Klaue, A.; Sponchioni, M.; Rossi, F.; Perale, G. A Methodologic Approach for the Selection of Bio-Resorbable Polymers in the Development of Medical Devices: The Case of Poly(L-Lactide-Co- $\epsilon$ -Caprolactone). *Polymers (Basel)*. **2018**, *10* (8), Article No. 851. <https://doi.org/10.3390/polym10080851>.
- (30) Manfredini, N.; Scibona, E.; Morbidelli, M.; Moscatelli, D.; Sponchioni, M. 110th Anniversary: Fast and Easy-to-Use Method for Coating Tissue Culture Polystyrene Surfaces with Nonfouling Copolymers to Prevent Cell Adhesion. *Ind. Eng. Chem. Res.* **2019**, *58*, 22290–22298. <https://doi.org/10.1021/acs.iecr.9b05104>.
- (31) Sponchioni, M.; Palmiero, U. C.; Moscatelli, D. HEMA-PEG Surfmers and Their Use in Stabilizing Fully Biodegradable Polymer Nanoparticles. *Macromol. Chem. Phys.* **2017**, *218* (23), 1–12. <https://doi.org/10.1002/macp.201700380>.
- (32) Grancaric, A. M.; Tarbuk, A.; Pusic, T. Electrokinetic Properties of Textile Fabrics. *Color. Technol.* **2005**, *121* (4), 221–227. <https://doi.org/10.1111/j.1478-4408.2005.tb00277.x>.
- (33) Sponchioni, M.; Capasso Palmiero, U.; Manfredini, N.; Moscatelli, D. RAFT Copolymerization of Oppositely Charged Monomers and Its Use to Tailor the Composition of Nonfouling Polyampholytes with an UCST Behaviour. *React. Chem. Eng.* **2019**, *4* (2), 436–446. <https://doi.org/10.1039/c8re00221e>.
- (34) Johnston, T. W. Summary of Experimental Results. *Rev. Laser Eng.* **1980**, *8* (1), 310–317. <https://doi.org/10.2184/lsej.8.310>.
- (35) Appell, L. Physical Foundations in Perfumery VIII. The Minimum Perceptible. In *Perfum. Cosmet.*; 1969; pp 45–50.



## Table of Contents



We optimize the design of polymer nanoparticles for fragrance delivery by studying how their physico-chemical properties affect adsorption on textile.